ELSEVIER

Journal of Alloys and Compounds 218 (1995) 51–57

Journal of ALLOYS AND COMPOUNDS

Changes of composition and surface state of palladium–nickel alloy gauzes used in ammonia oxidation apparatus

Zhenfen Yang *, Yuantao Ning, Huaizhi Zhao

Institute of Precious Metals, Kunming, Yunnan, 650221, People's Republic of China

Received May 4 1994; in final form 26 July 1994

Abstract

Pd–5Ni alloy was used as a capture gauze for platinum recovery in ammonia oxidation apparatus with a pressure of 4 atm (405 kPa) and a temperature of 850 °C. Chemical analysis, electron probe microanalysis and X-ray photoelectron spectroscopy were used to determine the changes and distribution of the compositions and the surface state of the gauze samples used for different times. The Pt/Pd and Rh/Pd ratios depend on the position of samples and the duration of the runs. The chemical species of major components on the surface of gauzes are Pd^0, PdO; Pt^0, PtO_{ads}, PtO_2; Rh_2O_3; Ni^0 and NiO. It was found that the Pt/Pd ratios on various surfaces of the gauzes are inversely proportional to the PdO concentration on the surfaces. A new mechanism of platinum recovery is discussed.

Keywords: Surface state; Composition change; Ammonia oxidation; Platinum recovery

1. Introduction

In the process for the preparation of nitric acid by ammonia oxidation, Pt–Rh and Pt–Pd–Rh alloys have been used as catalyst gauzes under the conditions of 1–10 atm pressure (101–1010 kPa) and temperatures of 800–950 °C. The platinum loss ratio of the gauzes reached 0.05–0.5 g of Pt per ton of HNO_3 in various nitric acid plants due to formation of the volatile oxide PtO_2 [1–5]. Pd–Au alloy capture gauzes were introduced and installed directly underneath the catalyst gauzes in order to recover the lost platinum [6–8]. In recent years, some metallic elements in Groups VIII and IB were recommended as substitutes for Au [9], and high-palladium alloys containing elements such as Cu or Ni and capture gauzes made of the alloys were developed [10,11].

The changes of the topography and chemical state of Pd–5Ni capture gauzes used at high pressures of 7–9 atm (709–912 kPa) and temperatures of 920–940 °C have been studied and reported [11]. In this work, the changes of the composition and surface state of Pd–5Ni alloy capture gauzes used at medium pressure (3–4 atm (304–405 kPa)) and temperature (850 °C) for different times were studied. According to the results, a new mechanism of platinum recovery by high-palladium alloy is proposed.

2. Experimental procedure

The capture pack consists of two sheets of Pd–5Ni alloy gauzes and three sheets of Fe–22Cr–5Al alloy gauzes as separator and sustainer. The pack was installed directly underneath Pt–Pd–Rh ternary alloy catalyst gauzes and was operated under conditions of 0.4 MPa pressure and a temperature of 850 °C in ammonia–air mixture containing 10.5–11.5% NH_3. The capture gauzes used for 5 and 8 months were named "W" and "T" gauzes, respectively. Samples were taken arbitrarily from the top (first) and bottom (second) gauzes. In the downstream direction, the various surfaces of samples were labelled a, b, c and d from the front surface of the top gauze to the back surface of the bottom gauze, and labelled W-a, W-b, W-c, W-d, T-a, T-b, T-c, T-d for the corresponding surfaces of W and T gauzes. Chemical analysis (CA), quantitative spectral analysis (inductively coupled plasma atomic emission spectrometry (ICP-AES)) and electron probe microanalysis (EPMA with Model 8705 instrument) were used to determine the concentrations of major components and impurities of the gauze samples. X-ray photoelectron spectroscopy (XPS with PHI 5600 ESCA system) was

* Corresponding author.

SSDI 0925-8388(94)01355-1

used to analyse the chemical state of the major elements on various surfaces in an ultra-high vacuum chamber with 5×10^{-10} Torr (6.66×10^{-8} Pa). Mg Kα radiation ($h\nu=1253.6$ eV) and the C 1s line at 284.8 eV were used as excitation source and charge reference to determine binding energies (*BE*) accurately, respectively. For quantitative calculations, the Pd 3d, Pt 4f, Rh 3d and Ni2P peak areas were computed assuming gaussian lines defined by their height and full width at half-maximum (FWHM). An Ar^+ spray was used to skin the surface with a 2 nm depth per minute.

3. Results

3.1. Composition changes of used Pd–5Ni capture gauzes

The contents of major components in new (N), W and T gauzes and those of the main impurities in T gauzes are listed in Tables 1 and 2, respectively. In the new gauzes, platinum and rhodium existed as impurities. In the gauzes used, platinum became the major component and the content of Rh also increased. The function of palladium alloy capture gauzes is platinum recovery. Comparing the Pt/Pd ratios of two sheets of gauzes, it is found that the Pt/Pd ratio of the top gauze is obviously higher than that of bottom gauze in both W and T gauzes and that the Pt/Pd ratio of two sheets of T gauzes used for 8 months is higher than that of corresponding W gauze used for 5 months. This means that the rate of platinum recovery, namely the ratio of recovered platinum by the capture gauze to platinum lost from catalyst gauze, of Pd–Ni capture gauzes increases with operating time. For example, the platinum recovery of T gauzes reached 73%, whereas that of W gauzes was only about 50%. Whether W or T gauzes are used, in addition, the platinum recovery of the first gauze is higher than that of the second gauze. On other hand, the Rh/Pd ratio on various gauze layers is much lower than the Pt/Pd ratio for both W and T gauzes. This is because the mass loss in catalyst gauzes is mainly that of platinum. In contrast to the tendency for changes of platinum or rhodium content, the Ni content of the gauzes used decreased gradually from 5 wt.% Ni in new gauzes to 0.17–0.18 wt.% in W gauzes and to 20–40 ppm in T gauzes. Moreover, the Ni content of the first gauze is obviously lower than that of second gauze. Although the concentration of some impurities such as Si, Fe, and Al in the dust collected from the surfaces of Pd–Ni gauzes is higher, the impurity contents of the gauzes themselves remain of the same order of magnitude as that of new gauze. The content of copper even decreased. This may be related to the oxidation and evaporation of Cu during usage similarly to that of Ni.

The average thickness of the various gauzes and the thickness ratio of the first sheet to the second sheet are given in Table 1. The thickness ratio increases with operating time. This indicates the possibility for improving gauze design, that is, the thickness, and thereby the platinum recovery, of the second layer of both W or T gauzes should increase on decreasing the mesh size of the first gauze. The contents of Pt, Pd and Rh on the sections of two sheets of T gauzes were determined by EPMA in order to establish their distribution. The Pt/Pd and Rh/Pd ratio calculated as a weight percentage are given in Fig. 1(c), in which a–d

Table 1
Changes of major components in N, W and T gauzes (wt.%)

Sample	Position	Pd	Pt	Rh	Ni	Pt/Pd	Rh/Pd	Gauze thickness (mm)	Gauze thickness (mm)
N	First sheet	95	0.011	0.0049	5	–	–	1.11	1.22
	Second sheet							0.09	
W	First sheet	65.18	33.18	0.46	0.18	0.51	7.1×10^{-3}	0.47	1.34
	Second sheet	89.05	9.43	0.31	1.17	0.11	3.5×10^{-3}	0.35	
T	First sheet	53.18	47.23	0.52	0.002	0.89	9.8×10^{-3}	0.75	1.67
	Second sheet	66.10	33.86	0.37	0.004	0.51	5.6×10^{-3}	0.45	

Table 2
Contents of main impurities in T gauzes (wt.%)

Sample	Position	Fe	Pb	Ag	Zn	Mg	Cu	Al	Si	Cr
N		0.0044	0.014	0.0018	0.0019	0.0002	0.0023	–	–	–
T	First sheet	0.0064	0.034	0.0013	0.0018	0.0013	<0.001	<0.001	0.0071	0.0042
	Second sheet	0.0066	0.043	0.0012	0.0012	0.001	<0.001	<0.001	0.0021	0.0038

Table 3
Pd 3d binding energy (eV) and concentration distribution of Pd and PdO on surfaces of N, W and T gauzes

Sample	Pd^0			PdO			Total content of Pd (at.%)
	$3d_{5/2}$	$3d_{3/2}$	Pd (at.%)	$3d_{5/2}$	$3d_{3/2}$	Pd (at.%)	
N	335.2			–	–	–	
W-a	335.15	340.43	50	–	–	–	50
W-b	335.29	340.54	45	337.0	342.22	23	68
W-c	335.24	340.55	48	337.05	342.36	28	76
W-d	–	–	–	337.10	342.35	88	88
T-a	335.27	340.57	40.36	337.08	342.33	7.70	48
T-b	335.28	340.66	35.88	337.05	342.33	34.30	70
T-c	335.27	340.55	48.63	336.94	342.12	20.71	69.3
T-d	335.22	340.50	42.40	337.05	342.38	37.19	79.59

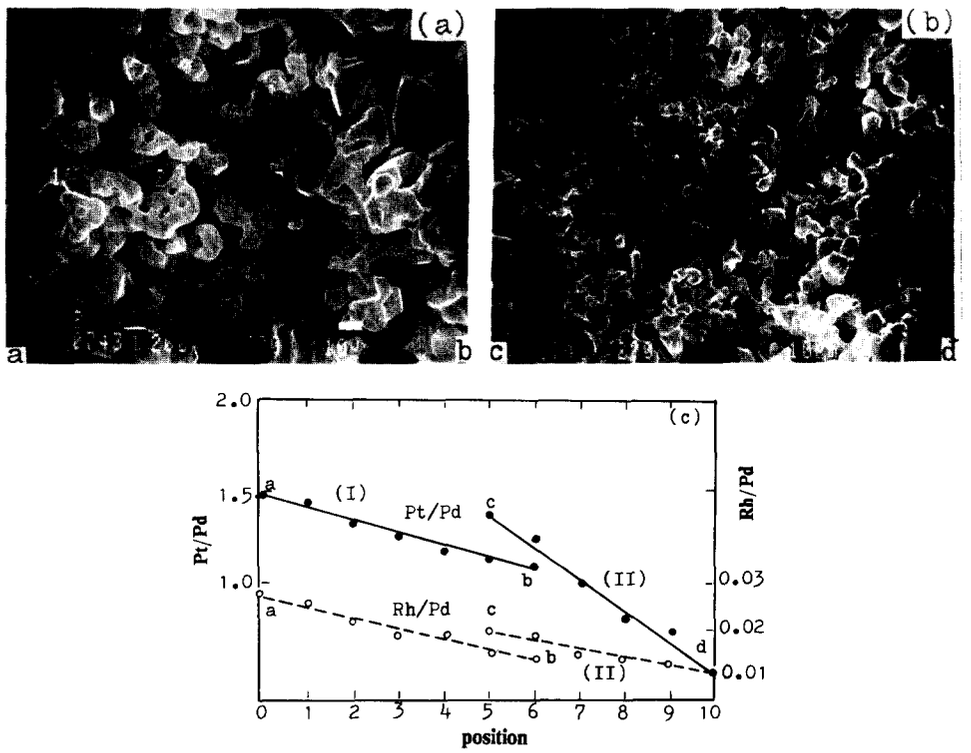

Fig. 1. Topography (a), (b) and distribution of Pt/Pd and Rh/Pd ratio (c) in sections of first (I) and second sheet (II) of T gauzes.

denote the four different surfaces and the points 1–9 are illustrated by means of Fig. 1(a) and (b). The Pt/Pd and Rh/Pd ratios of the a and c surfaces are higher than those of b and d surfaces. This is because the Pt and Rh lost from the catalyst gauzes are deposited preferentially on the surfaces. In other words, the front surfaces facing on the stream have a higher Pt recovery than back surfaces due to gas transportation. It can also be seen from Fig. 1(c) that the slope of Pt/Pd ratio in section I is obviously lower than that in section II. This reflects that the diffusion rate of Pt in section I is higher than that in section II. The slopes of the Rh/Pd ratio in both sections, however, are essentially the same. This is related to the deposition of Rh in the form of Rh_2O_3 particles.

3.2. Surface composition and chemical states of Pd–5Ni capture gauzes

Pd species and their distribution

The chemical states of Pd in N, W and T gauzes were determined by XPS, and the Pd 3d XPS profiles are shown in Fig. 2. Obvious shoulder peaks can be observed with XPS on various surfaces except the N gauze and also W-a and W-d surfaces. Here the XPS profiles show only a single peak. The binding energies (*BE*) of Pd $3d_{5/2}$ and $3d_{3/2}$ are given in Table 3. The

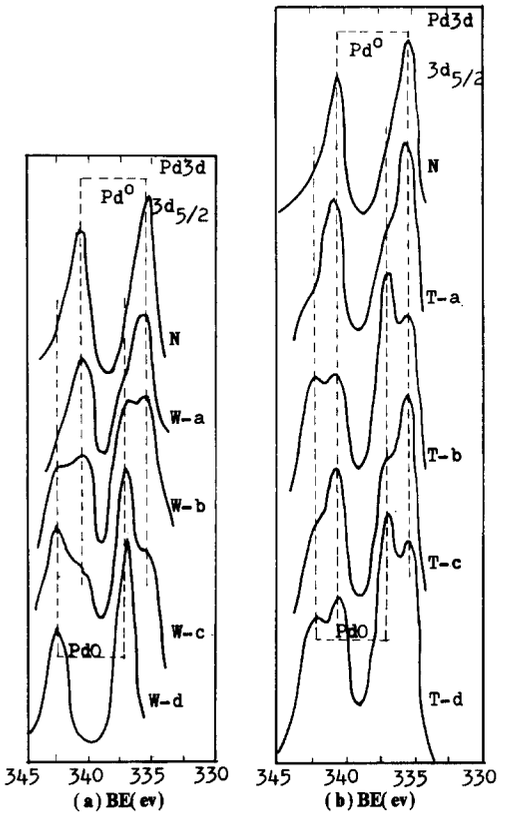

Fig. 2. Pd 3d XPS on surfaces of N, W and T gauzes.

BE of Pd $3d_{5/2}$ in the range 335.15–335.29 eV is in accord with *BE* data (335 eV) for Pd^0 in the literature [12,13]. Although the *BE* in the range 336.94–337.10 eV differs by about 0.7 eV from the literature data (336.3 eV) for PdO [12,13], we did find PdO in the XRD spectrum of W gauzes. In addition, the Pd $3d_{5/2}$ *BE* values for PdO powders prepared in a strong oxygen atmosphere using different methods are in the range 337 ± 0.2 eV [14]. The above results indicate clearly the presence of two Pd chemical species, Pd^0 and PdO, on the surfaces of the gauzes.

The concentrations of Pd and PdO calculated from the individual peak area are given in Table 3. No PdO species was found in the N gauze because its wires were annealed in high-purity argon. The single chemical species Pd^0 on the W-a and PdO on the W-d surface were observed. It can be seen from Table 3 that the Pd^0 concentrations on surfaces a and c facing the stream are higher than those on surfaces b and d, whereas the PdO concentrations on the former are lower than those on the latter (Fig. 3). After peeling off the W-d surface for 3 min with an Ar^+ spray, the PdO spectrum in XPS disappeared, indicating that PdO species exists only in the surface with a depth of less than 6 nm.

Pt species and their distribution

The Pt 4f XPS profiles are shown in Fig. 4. The FWHM of the Pt $4f_{7/2}$ and $4f_{5/2}$ peaks and the height

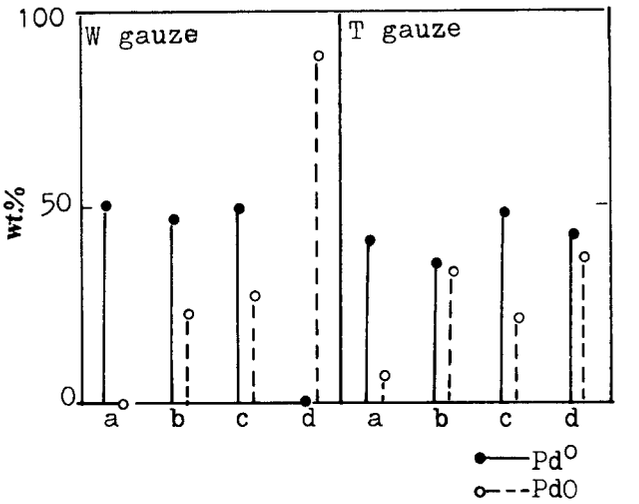

Fig. 3. Distribution of Pd^0 and PdO on various surfaces of W and T gauzes.

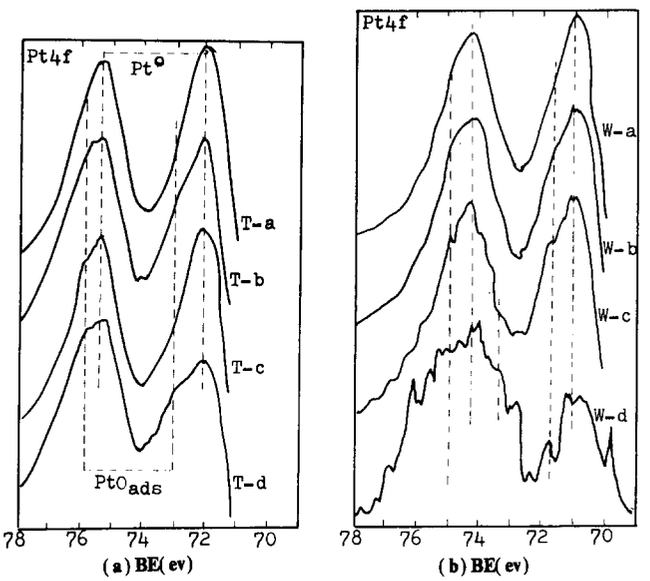

Fig. 4. Pt4f XPS on W and T gauzes.

of the $4f_{5/2}$ peaks increase gradually from surface a to d. The peaks obviously show asymmetry and incline to the side of high energy. The area ratio of the $4f_{7/2}$ and $4f_{5/2}$ peaks is less than the theoretical value of 1.33, which indicates the existence of platinum oxide. The Pt $4f_{7/2}$ *BE* values given in Table 4 are in agreement with the literature data for Pt^0 (*BE* = 70.7–71.15 eV) and PtO_{ads} (*BE* = 71.8 eV) [12,15], indicating the presence of Pt^0 on various surfaces and of PtO_{ads} on the surfaces except W-a and T-a. In addition, a separated peak with *BE* = 74.26 eV which corresponds to that of PtO_2 species was observed in the Pt $4f_{7/2}$ XPS profile of the W-d surface. This result is in accordance with that observed by Fierro et al. [11] at the outlet Pd gauzes in a high-pressure ammonia oxidation plant. Similarly to PdO species, the depth of oxidized Pt species including PtO_{ads} and PtO_2 is less than 6 nm,

Table 4
Pt $4f_{7/2}$ *BE* values (eV) on various surfaces of W and T gauzes

Surface	Pt^0	PtO_{ads}	PtO_2	Total content of Pt (at.%)
W-a	70.97	–	–	32.8
W-b	70.88	72	–	24
W-c	70.96	71.92	–	20.2
W-d	70.65	71.92	74.26	5.3
T-a	70.97	–	–	34
T-b	71.02	72.23	–	15
T-c	70.92	71.68	–	14.2
T-d	70.91	72.53	–	10.5

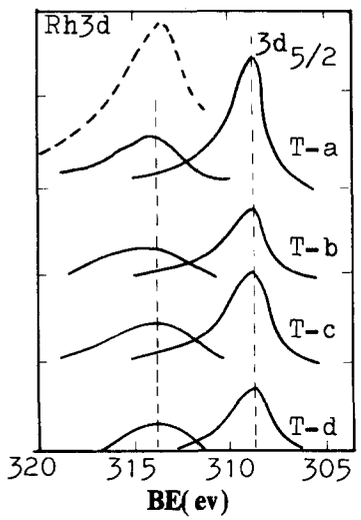

Fig. 5. Rh3d XPS on T gauzes.

as determined with an Ar^+ spray for 3 min to peel the W-d surface.

Rh species and their distribution

The Rh 3d XPS profiles on the surfaces of T gauzes are shown in Fig. 5. The dashed peak is superimposed on the Pt 4d peak, which causes higher intensities of $3d_{3/2}$ than $3d_{5/2}$ peaks. The solid peaks are the separated Rh $3d_{5/2}$ and $3d_{3/2}$ peaks. They are located at 308.55 and 313.60 eV (Table 5), respectively. The former corresponds to the data reported for Rh_2O_3 $3d_{5/2}$ (*BE* = 308.2, 308.8 eV) [1,12]. The Rh species was not found either before or after an Ar^+ spray on various surfaces. This indicates the presence of Rh in the form of Rh_2O_3. Rh-rich particles containing 80–83 wt.% Rh were found by EPMA on the surfaces of T gauzes. The Rh content corresponds to that in the Rh_2O_3 molecule, further confirming the existence of Rh as Rh_2O_3.

Ni species and their distribution

No Ni was found by XPS analysis on the various surfaces of the T gauzes or on the W-a and W-b surfaces. Ni 2p XPS occurred only on the W-c and W-d surfaces. The Ni $2p_{3/2}$ *BE* of 855.76 eV (Table 6) is in the upper limit of NiO (853–856 eV) and the lower limit of Ni_2O_3 (855.8–857.3 eV) reported in the literature [12,16–20]. On the other hand, two diffraction peaks with *d*-spacing values of 0.2086 and 0.1475 nm observed in the XRD patterns of W-c and W-d surfaces correspond to the (200) and (220) planes of NiO. This means that the Ni oxide on the W-c and W-d surfaces is NiO. The slightly higher *BE* values of PdO and NiO measured in this work may be due to the different calibrations of the spectrometers or to the use of the C 1s line with *BE* 284.8 eV as a reference material. After peeling the W-d surface with an Ar^+ spray for

Table 5
Rh 3d *BE* values (eV)

Surface	Rh_2O_3		Content of Rh (at.%)
	$3d_{7/2}$	$3d_{5/2}$	
W-a	308.42	313.67	11.27
W-b	308.45	313.70	6.12
W-c	–	–	–
W-d	–	–	–
T-a	308.55	313.8	18.18
T-b	308.71	313.78	11.17
T-c	308.70	313.82	16.52
T-d	308.73	313.48	9.98

Table 6
$Ni2p_{3/2}$ *BE* values (eV)

Sample	Ni^0	NiO	Ni (at.%)
W-c	–	855.76	2.74
W-d	–	855.76	6.90
W-d	852.73	–	9.76 (sprayed for 3 min) [a]
W-d	852.73	–	10.12 (sprayed for 6 min) [a]

[a] A 1 min spray corresponds to a depth of 2 nm.


Fig. 6. Topography of W–d surface and porous structure of Pd gauze.

3–6 min the NiO spectrum disappeared and Ni^0 species occurred in the internal layers with a 9–10 at.% Ni content, which is close to the original Ni content (5 wt.%). As the Ni bulk content of the second W gauzes was only 1.17 wt.% (Table 1), this clearly indicates nickel enrichment at the surface layer.

Fig. 6(a) shows the topography of the W-d surface. The Pd content on the surface reaches 90 wt.%, which corresponds to the Pd content in PdO. This means that the surface is covered by PdO. The Ni content in the catkin-like matter around the surface reaches 50–77 wt.%. The catkin consists of NiO in addition to small amount of oxides of other metals such as Pd, Pt, Al, Fe and Cr. The catkin matter was formed through volatilization and accumulation of NiO, and was finally carried away through the stream. Ni inside the gauzes diffused to the surface and was oxidized continuously. This led to the Ni content in the gauze decreasing gradually until the Ni solute disappeared completely, as shown in Table 1. It is likely that the other base metal additives or impurities undergo a similar oxidation process, which is the reason why their contents remained very low in the used capture gauzes.

4. Discussion

From these studies on the changes of composition and surface state in capture gauzes made of high-palladium alloy, we are of the opinion that the platinum recovery process includes generally the following processes: (1) the volatile platinum oxide, PtO_2, formed in Pt–Rh or Pt–Pd–Rh catalytic gauzes is transported to the capture gauzes by the stream; (2) PtO_2 is reduced to Pt; (3) Pt deposits on the surfaces of the capture gauzes and diffuses inwards; and (4) new Pd(Pt) solid solution crystals form and grow. The last process will be considered in some detail in another paper [21]. Here we discuss only the reduction mechanism of PtO_2. Obviously, the mechanism is related to the surface state of Pd under the operating conditions.

The heated palladium forms a PdO film at 348 °C on the surface, and the film thickness increases with increase in temperature. At 750 °C, PdO decomposes by a reversible reaction $2PdO \rightarrow 2Pd + O_2$ [22]. In addition, Pd metal volatilizes at high temperature owing to the increased vapour pressure. Hence the surface of palladium is a multilayer structure above 800 °C: the bright Pd-metal surface is covered by a thin layer of Pd-metal vapour, which is covered by PdO vapour [23]. PtO_2 vapour is transported by the stream to the surface of Pd alloy capture gauzes and comes into contact with PdO vapour. Because the affinity of Pd to oxygen is stronger than that of Pt, the Pd released by the PdO decomposition reacts with PtO_2 and reduces PtO_2 to Pt: $2PdO \rightarrow 2Pd + O_2$, $2Pd + PtO_2 \rightarrow Pt + 2PdO$. Of course, Pd-metal vapour is likely to participate in the reaction. The reduced Pt deposits immediately on the bright surface of the Pd metal and forms a solid solution. The process is shown schematically in Fig. 7. According to Fig. 1(c) and Table 3, the Pt/Pd ratio is inversely proportional to the PdO concentration for various surfaces of T gauzes, as shown in Fig. 8. Comparing the corresponding data listed in Tables 1 and 3, this inverse proportional tendency is also found on W gauzes. This clearly indicates that PdO participates in the reduction of PtO, which leads to a decrease in PdO concentration. As further evidence for this mechanism, we believe that the porous structure (Fig. 6) of Pd gauzes formed in the operating period was caused by the oxygen released during PdO decomposition and PtO_2 reduction, but not by the external stream. On the other hand, the PdO concentration of a surfaces of both W and T gauzes is zero or very low. This indicates that the reduction reaction of PtO_2 on surface a has reached completion. On the other surfaces, the reaction may be incomplete, such as $PtO_2 + Pd \rightarrow PtO + PdO$, the formed PtO being adsorbed on the surfaces.

The mechanism can explain why Pd and high-palladium alloys have the highest platinum recovery. It is because the reduction effect of Pd to PtO_2 and the characteristics of Pd leading to a bright metal surface at high temperature are unique. Although Pt and Au also give rise to bright metal surfaces at high temperature, experiments indicated that their platinum

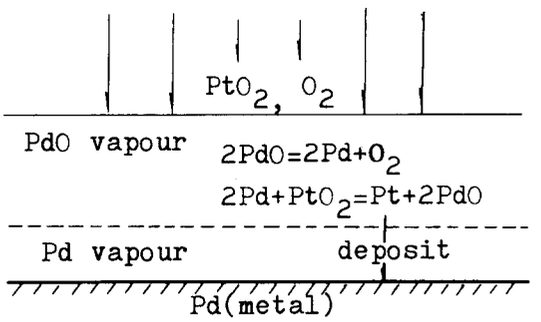

Fig. 7. The multilayer structure of Pd and PtO_2 being reduced.

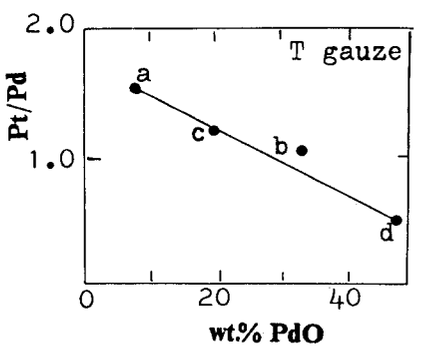

Fig. 8. Pt/Pd ratio is inversely proportional of PdO concentration on various surfaces of T gauzes.

recovery was much lower than that of palladium [7]. This is because the Au surface does not have the ability to reduce PtO_2, whereas Pt still forms PtO_2 at the operating temperature of the capture gauze. Other metals, such as Ni, Cu and Fe, are not suitable as capture gauzes because they are quickly oxidized and disappear under strong oxidizing atmospheres, so the high platinum recovery rate of Pd and high-Pd alloys is related to the oxidation characteristics and surface structure of palladium at high temperature. Of course, the mechanism does not reject the partial reduction reaction of remaining NH_3 to PtO_2 [11]. Even if the PtO_2 is reduced by the NH_3 in the stream, the reduced Pt should be oxidized immediately by the remaining O_2.

The Rh_2O_3 particles formed on the catalyst gauzes are deposited mechanically on the surfaces of the capture gauzes by the stream. Because Rh_2O_3 is more stable than PdO, it cannot be reduced by Pd.

It can be seen from the analysis data for Ni that the loss of Ni is gradual. The Ni solute in capture gauzes disappeared completely. Hence Ni did not contribute to the platinum recovery of Pd capture gauzes, it only strengthened the original palladium alloy. A higher Ni content would decrease further the platinum recovery. In this work, Pd–40Ni alloy capture gauzes were used for about 8 months under the same condition. The Pt recovery rate, only 32%, was much lower than that of T gauzes, The surfaces of high-Ni gauzes were covered by an NiO film, which made the surfaces of the capture gauzes lose the multilayer structure characteristic of palladium.

5. Conclusions

The composition and chemical species of the Pd–5Ni alloy capture gauzes used in ammonia oxidation apparatus under medium pressure obviously changed before and after usage. The chemical species of major components on the surfaces are Pd^0, PdO; Pt^0, PtO_{ads}, PtO_2; Rh_2O_3; Ni and NiO. The thickness of the oxides is generally less than 6 nm. The Pt/Pd ratio of a gauze is related to its position in the capture gauze pack: the ratio of the top gauze is higher than that of the bottom gauze, and that of the front surface facing the stream is higher than that of the back surface. Also, the Pt/Pd ratio on various surfaces is inversely proportional to the PdO concentration of the surfaces. Rh_2O_3 is present in the form of particles. The Ni solute diffuses to the surface and is oxidized to form NiO, and finally disappears completely. The platinum recovery process includes adsorption, reduction, deposition, alloying and recrystallization. The high platinum recovery rate of Pd or high-Pd alloy capture gauzes is related to the unique oxidation characteristics and surface structure of palladium.

Acknowledgement

This project (59271027) was supported by the National Natural Science Foundation of China.

References

[1] J.P. Contour, G. Mouvier, M. Hoogewys and C. Leclere, *J. Catal., 48* (1977) 217.
[2] A.R. McCabe and G.D.W. Smith, *Platinum Met. Rev., 32* (1988) 11.
[3] J.L.G. Fierro, J.M. Palacios and F. Tomas, *Surf. Interface Anal., 13* (1988) 25.
[4] M. Rubel, M. Pszonicka and W. Palczewska, *J. Mater. Sci., 20* (1985) 3639.
[5] M. Rubel and M. Pszonicka, *J. Mater. Sci., 21* (1986) 241.
[6] H. Holzmann, *Platinum Met. Rev., 13* (1969) 2.
[7] A.E. Heywood, *Plainum Met. Rev., 17* (1973) 118.
[8] A.E. Heywood, *Platinum Met. Rev., 26* (1982) 28.
[9] R.W. Hatfield, B.S. Beshty, H.C. Lee, R.M. Heek and T.S. Hsing, *European Patent,* 077121, 1982.
[10] J.L.G. Fierro, J.M. Palacios and F. Tomás, *Platinum Met. Rev., 34* (1990) 62.
[11] J.L.G. Fierro, J.M. Palacios and F. Tomás, *Surf. Interface Anal., 14* (1989) 529.
[12] F.M. John, *Handbook of X-Ray Photoelectron Spectroscopy,* Perkin-Elmer Physical Electronics Division, Eden Prairie, MN, 1992.
[13] K.S. Kim, A.F. Gossmann and N. Winograd, *Anal. Chem., 46* (1974) 197.
[14] Z.-F. Yang, Y.-T. Ning and H.-Z. Zhao, to be published.
[15] K.S. Kim, N. Winograd and R.E. Davis, *J. Am. Chem. Soc., 93* (1971) 6296.
[16] N.S. McIntyre and M.G. Cook, *Anal. Chem., 47* (1975) 2208.
[17] K.T. Ng and D.M. Hercules, *J. Phys. Chem., 80* (1976) 2095.
[18] T. Dickinson, A.F. Povey and P.M.A. Sherwood, *J. Chem. Soc., Faraday Trans., 73* (1977) 332.
[19] P. Lorenz, J. Finster, G. Wendt, J.V. Salyn, E.K. Zumadilov and V. Nefedov, *J. Electron Spectrosc. Relat. Phenom., 16* (1979) 267.
[20] R.B. Shalvog, P.J. Reucroft and D.H. Davis, *J. Catal., 56* (1979) 336.
[21] Y. Ning, Z. Yang and H. Zhao, *Platinum Met. Rev., 39* (1995) 9.
[22] M.P. Slavensky, *Physico-chemical Properties of Elements,* Metallurgiya, Moscow, 1952 (in Russian).
[23] J.C. Chaston, *Platinum Met. Rev., 9* (1965) 126.